Direct observations of a Mt Everest snowstorm from the world's highest surface-based radar observations

L. Baker Perry[1], Sandra E. Yuter[2], Tom Matthews[3], Patrick Wagnon[4], Arbindra Khadka[5,6], Deepak Aryal[5], Dibas Shrestha[5], Alex Tait[7], Matthew A. Miller[2], Alex O'Neill[1], Spencer R. Rhodes[2], Inka Koch[6], Tenzing G. Sherpa[8], Subash Tuladhar[9], Saraju K. Baidya[9], Sandra Elvin[7], Aurora C. Elmore[7], Ananta Gajurel[5] and Paul A. Mayewski[10]

[1]*Appalachian State University, Boone, North Carolina, USA*
[2]*North Carolina State University, Raleigh, North Carolina, USA*
[3]*Loughborough University, Loughborough, UK*
[4]*University Grenoble Alpes, CNRS, IRD, IGE, Grenoble, France*
[5]*Tribhuvan University, Kirtipur, Nepal*
[6]*ICIMOD, Patan, Nepal*
[7]*National Geographic Society, Washington, USA*
[8]*Khumbu Climbing Center, Khumjung, Nepal*
[9]*Department of Hydrology and Meteorology, Kathmandu, Nepal*
[10]*University of Maine, Orono, Maine, USA*

In April and May 2019, National Geographic and Rolex's Perpetual Planet Expedition to Mt Everest (hereafter 2019 Everest Expedition) undertook the most comprehensive science expedition to the Khumbu (Mt Everest) region and included teams of scientists investigating a range of topics, including glacier change, upward shifts in ecosystems, black carbon deposition on glacier surfaces and snow/ice/water chemistry (Mayewski *et al*., 2020). As the highest mountain on Earth and the heart of the Himalayan water tower supplying water to hundreds of millions of people (Pritchard, 2019; Immerzeel *et al*., 2020), the rate and impacts of climate change on Mt Everest (known in Nepal and China as *Sagarmatha* and *Qomolangma*, respectively) are of tremendous symbolic and practical significance. Weather conditions on Mt Everest are also a key component of climber safety (Moore and Semple, 2004, 2006; Moore *et al*., 2010).

The extreme environment has challenged data collection and limited past insights. For example, prior to the 2019 Everest Expedition, which installed five automatic weather stations, including the two highest in the world (Matthews *et al*., 2020), direct weather observations were absent from the upper 3500m of the mountain, despite the recognition that data from these elevations can improve understanding of the Himalayan hydrological cycle and improve monitoring of upper-atmosphere winds. Other regional networks are available, although sparse (Sherpa *et al*., 2017; Litt *et al*., 2019), including those operated by the Institute for Development Research (France) and Tribhuvan University (e.g. the Mera Peak station, at 6400m asl, is located 30 km south of Mt Everest). Process insights into hydrological cycling were also sought through deployment of the highest elevation vertically pointing 24GHz Micro Rain Radar (Peters *et al*., 2005) at 5280m asl at Nepal's Everest Base Camp. This paper details the first continuous observations of the vertical structure of a snowstorm in the Khumbu region on 17 April 2019 (Figure 1).

Snow began falling at ~1200 UTC on 16 April 2019 and continued through 1700 UTC 17 April 2019 in association with a 500hPa trough upstream over northern India with moist southwest flow (not shown). The team arrived at the Everest Base Camp at approximately 0600 UTC 17 April 2019 and immediately deployed the Micro Rain Radar (Figure 2), a manual precipitation gauge and a snow board in anticipation of additional snowfall. We recorded 9.2mm liquid-equivalent precipitation (9.5cm snowfall) from a core sample collected on a snow board ending at 1800 UTC 17 April 2019 at the Everest Base Camp, which does not include snowfall from the previous day. The nearby Institute for Development Research and Tribhuvan University weather stations reported liquid-equivalent precipitation (corrected for undercatch using available wind speed data following Wagnon *et al*., 2009) of 10.7mm at Pyramid (5050m asl and ~8km southwest) and 5.1mm at Pheriche (4240m asl and ~13km south-southwest) ending at 1800 UTC 17 April 2019. Further down valley, our recently installed weather station at Phortse (3810m asl and ~20km southwest: Matthews *et al*., 2020) that includes a double-alter shielded weighing precipitation gauge recorded 7.0mm precipitation during the same time period. Available surface observations of wind speed and direction during the storm showed channelled upslope flow of ~2–6ms^{-1} through the valleys during the day, a common occurrence in the Khumbu region (Bollasina *et al*., 2002; Bonasoni *et al*., 2010).

Micro Rain Radar time–height profiles of radar reflectivity, spectral width (a proxy for turbulence) and Doppler velocity indicate two main episodes of snow on 17 April 2019 (Figure 3). The observed precipitation and velocity structures are similar to those observed by the Micro Rain Radar in snowstorms in other mountainous areas, including Boone, NC and Alta, UT in the USA (Keighton *et al*., 2009; Garrett *et al*., 2015) and the tropical Andes of Peru and Bolivia (Endries *et al*., 2018). Surface visual observations indicated that most of the snow fell as a mixture of graupel and aggregates that included particles with light to moderate riming. Pristine ice crystals were not observed at the surface. A higher percentage of graupel was noted close to 0800 UTC. After a few minutes of snow at 0700 UTC, a longer period of more intense snow fell from 0750 UTC to 1110 UTC, and a second period of snow fell from 1300 UTC to 1517 UTC. The closest weather station recording at the time was Changri Nup (located on a debris-free glacier at 5387m asl and ~7km west-southwest), where air temperature ranged from –3°C to –7°C, and relative humidity was between 80% and 90% during the snowfall.

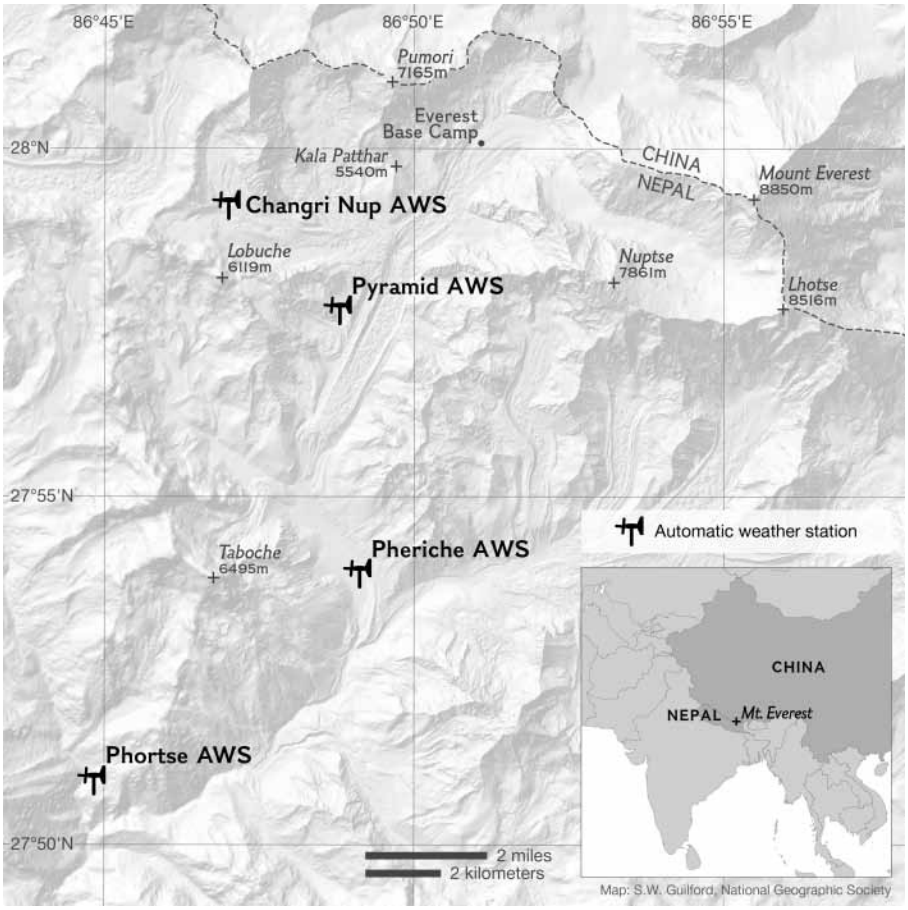

Figure 1. Topographic map of Khumbu region showing locations of Nepal's Everest Base Camp and weather stations at Phortse, Pheriche, Pyramid and Changri Nup as well as altitudes of nearby peaks. Inset map shows location of Mt Everest on the border of Nepal and China.

Figure 2. Photos from 17 April 2019 showing (a) the approach to Everest Base Camp at 0450 UTC; (b) Micro Rain Radar deployment at Everest Base Camp at 0633 UTC; and (c) falling snow at 0906 UTC, including graupel and large aggregate particles. (Photo credits: L.B. Perry/ National Geographic.)

Echo tops reached as high as 4500m above ground level (9780m asl), and most of the echo was within 3000m of ground level or between 5280 and 8280m asl. Weather radar detects precipitation-sized particles >0.2mm in diameter, so the echo top is usually lower than the cloud top (which may consist of cloud droplets <0.2mm). The relationships among radar reflectivity, spectral width and Doppler velocity were variable throughout the snow event (Figure 3). Radar reflectivity is roughly proportional to $\log_{10}(\text{mass}^3)$ in snow and is a time-integrated quantity representing snow particles that formed at different times and locations but ended up in the same volume of air. Reflectivity values ranged from the minimum detectable value of 0dBZ to 25dBZ. Higher spectral width ($>1 ms^{-1}$) is an indicator of greater turbulence (e.g. 1030 UTC to 1045 UTC) and favourable locations for riming (Garrett *et al*., 2015). Both upward and downward motions were evident in Doppler velocity as the storm passed over the Everest Base Camp. Measured Doppler velocity is the sum of the vertical air motions and precipitation fall speed. Fall speeds for aggregates and graupel are typically $\sim 1 ms^{-1}$ (Garrett and Yuter, 2014). The upward (negative) values of Doppler velocity indicate updrafts up to $2 ms^{-1}$ and localized pockets of instability. Pockets of upward air motions are likely locations of precipitable snow mass growth within the storm, and many of these were near the echo top. Downward (positive) values of Doppler velocity are the result of a combination of downward air motions and downward fall speeds. The higher downward Doppler velocity values sometimes occurred with high reflectivities (e.g. 0800 UTC and 0840 UTC) and sometimes did not (e.g. 0856 UTC to 0918 UTC). A power surge at the Everest Base Camp the following day damaged the Micro Rain Radar and prevented additional measurements during the 2019 Everest Expedition.

At times, the observed snowstorm extended higher (9780m asl) than the elevation of Mt Everest (8850m asl per updated guidance from National Geographic) suggesting that new snow accumulation on the summit was possible, and cloud immersion was likely. However, most of the time, snowfall was confined to altitudes below the summit. The radar echo contained both upward and downward motions, as well as episodes of higher spectral width indicative of turbulence and environments favourable for riming. These unique vertically pointing radar measurements represent the highest altitude snowstorm ever directly measured from the surface. Although there are lower air pressures at the Everest Base Camp (~530hPa) compared to mountain snowstorms at lower elevations, the structure of the storm is not noticeably different; typical snowstorm structures and their heights above ground level are instead displaced higher relative to sea level. Observations of this single event suggest that satellite-based remote sensing of snowstorms can utilise assumptions of similar structures across a range of mountain elevations.

Acknowledgments

This research was conducted in partnership with the National Geographic Society, Rolex and faculty and students of Tribhuvan University, with approval from all relevant agencies of the Government of Nepal. We thank the communities of the Khumbu Region, our expedition support team, Shangri-La Nepal Trek, Pete Athans

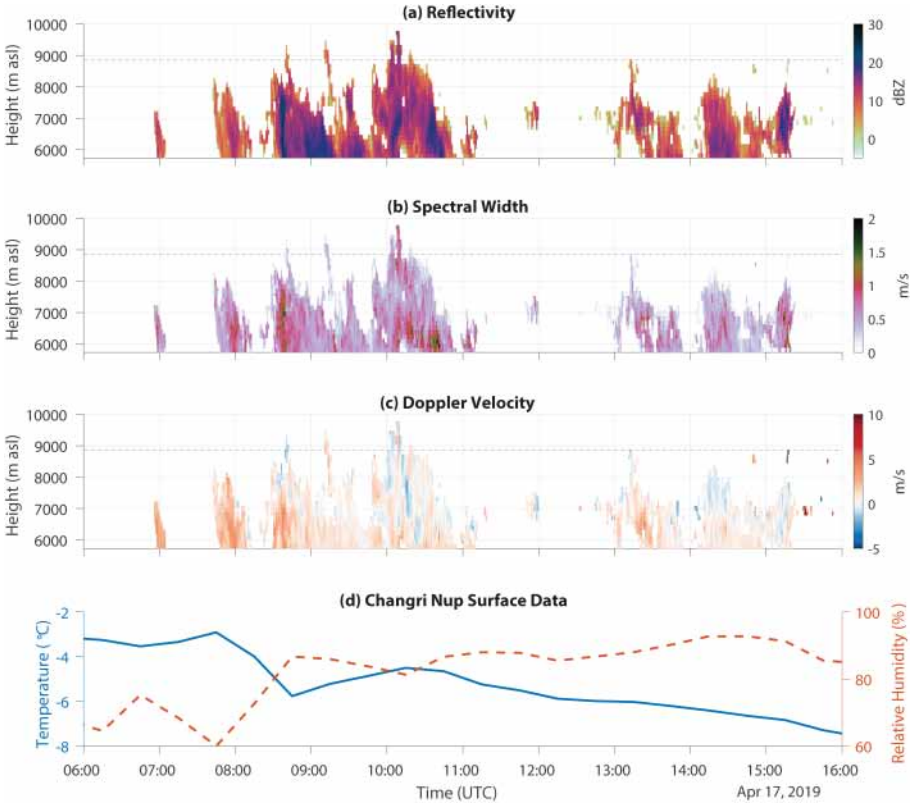

Figure 3. Observations from 0600 to 1600 UTC on 17 April 2019 showing (a) reflectivity, (b) spectral width and (c) Doppler velocity time height plots from Micro Rain Radar at the Everest Base Camp (5280m asl) along with (d) surface observations of temperature (solid blue line) and relative humidity (dashed orange line) from nearby Changri Nup weather station (5387m asl and ~7km west-southwest). Regional sunset occurred at 1239 UTC; Nepal local time is UTC +0545. The dashed line in panels (a), (b) and (c) indicates the height of Mt Everest (8850m asl).

and Conrad Anker. We are grateful for Sam Guilford's assistance in preparing Figure 1 and Toby Peele's assistance in preparing Figure 3. Additional funding supporting this research was provided by the National Science Foundation through Grants AGS-1347179 (Perry) and AGS-1905736 (Yuter, Miller, and Rhodes). Changri Nup, Pyramid and Pheriche stations have been funded by the French Service d'Observation GLACIOCLIM (part of IR OZCAR) and by a grant from Labex OSUG@2020 (Investissements d'avenir – ANR10 LABX56) and have been operated with the support of the JEAI HIMALICE and the Ev-K2-CNR Project in collaboration with the Nepal Academy of Science and Technology and Tribhuvan University. We are grateful for the helpful feedback from G.W.K. Moore and an anonymous reviewer.

References

Bollasina M, **Bertolani L**, **Tartari G**. 2002. Meteorological observations at high altitude in Khumbu Valley, Nepal Himalayas, 1994–1999. *Bull. Glaciol. Res.* **19**: 1–11.

Bonasoni P, **Laj P**, **Marinoni A** ***et al***. 2010. Atmospheric Brown Clouds in the Himalayas: first two years of continuous observations at the Nepal Climate Observatory-Pyramid (5079 m), Atmos. *Chem. Phys.* **10**: 7515–7531.

Endries JL, **Perry LB**, **Yuter SE** ***et al***. 2018. Radar-observed characteristics of precipitation in the tropical high Andes of southern Peru and Bolivia. *J. App. Met. Clim.* **57**: 1441–1458.

Garrett TJ, **Yuter SE**. 2014. Observed influence of riming, temperature, and turbulence on the fallspeed of solid precipitation. *Geophys. Res. Lett.* **41**: 6515–6522.

Garrett TJ, **Yuter SE**, **Fallgatter C** ***et al***. 2015. Orientations and aspect ratios of falling snow. *Geophys. Res. Lett.* **42**: 4617–4622.

Immerzeel WW, **Lutz AF**, **Andrade M** ***et al***. 2020. Importance and vulnerability of the world's water towers. *Nature* **577**: 364–369.

Keighton S, **Lee L**, **Holloway B** ***et al***. 2009. A collaborative approach to study northwest flow snow in the southern Appalachians. *Bull. Amer. Meteor. Soc.* **90**: 979–991.

Litt M, **Shea J**, **Wagnon P** ***et al***. 2019. Glacier ablation and temperature indexed melt models in the Nepalese Himalaya. *Sci. Rep.* **9**: 5264.

Matthews T, **Perry LB**, **Koch I** ***et al***. 2020. Going to extremes: installing the world's highest weather stations on Mount Everest. *Bull. Am. Meteorol. Soc.* **101**: E1870–E1890.

Mayewski PW, **Gajurel A**, **Elvin S** ***et al***. 2020. Pushing climate change science to the roof of the world. *One Earth* **3**: 556–560.

Moore GWK, **Semple JL**. 2004. High Himalayan meteorology: weather at the South Col of Mount Everest. *Geophys. Res. Lett.* **31**: L18109.

Moore GWK, **Semple JL**. 2006. Weather And Death On Mount Everest: An Analysis Of The Into Thin Air Storm. *Bull. Am. Meteorol. Soc.* **87**: 465–480.

Moore GK, **Semple JL**, **Sikka DR**. 2010. Mallory and Irvine on Mount Everest: Did extreme weather play a role in their disappearance? *Weather* **65**(8): 215–218.

Peters G, **Fischer B**, **Münster H** ***et al***. 2005. Profiles of raindrop size distributions as retrieved by microrain radars. *J. Appl. Meteorol.* **44**: 1930–1949.

Pritchard HD. 2019. Asia's shrinking glaciers protect large populations from drought stress. *Nature* **569**: 649–654.

Sherpa SF, **Wagnon P**, **Brun F** ***et al***. 2017. Contrasted surface mass balances of debris-free glaciers observed between the southern and inner parts of the Everest region (2007-15). *J. Glaciol.* **63**: 637–651.

Wagnon P, **Lafaysse M**, **Lejeune Y** ***et al***. 2009. Understanding and modelling the physical processes that govern the melting of the snow cover in a tropical mountain environment in Ecuador. *J. Geophys. Res.* **114**: D19113.

Correspondence to: L. B. Perry

perrylb@appstate.edu

doi: 10.1002/wea.3854